

1990-290000

## A DISCRETE DECENTRALIZED VARIABLE STRUCTURE ROBOTIC CONTROLLER

*Zuheir S. Tumei*

School of Electrical Engineering  
Georgia Institute of Technology  
Atlanta, Georgia, 30332  
Tel. (404) 894-3812

### Abstract :

In this paper a decentralized trajectory controller for robotic manipulators is designed and tested using a multiprocessor architecture and a PUMA 560 robot arm. The controller is made up of a nominal model-based component and a correction component based on a variable structure suction control approach. The second control component is designed using bounds on the difference between the used and actual values of the model parameters. Since the continuous manipulator system is digitally controlled along a trajectory, a discretized equivalent model of the manipulator is used to derive the controller. The motivation for decentralized control is that the derived algorithms can be executed in parallel using a distributed, relatively inexpensive, architecture where each joint is assigned a microprocessor. Nonlinear interaction and coupling between joints is treated as a disturbance torque that is estimated and compensated for.

### 1. Introduction :

Strategies for designing manipulator controllers can generally be classified according to the degree of their dependence on the availability of reasonably accurate manipulator models. While some of these schemes, such as those based on systems with variable structure [1-10], model referenced [11,12], and self tuning controllers [13,14], are not necessarily model-based, others [15-22] depend to a varying extent on the availability of such models. Although controllers that belong to the first class are clearly robust to model inaccuracies, such schemes often disregard useful information embodied in the dynamic equations. Some of these approaches, however, have recently taken account of manipulator dynamics [2,4,5,11,12,22] in the form of additional nonlinear feedback. Model-based robot controllers, on the other hand, such as the computed torque control [15], are susceptible to deviations of the used model parameters from their actual values. More general nonlinear model-based control approaches [16,17] rely on using the complicated Lagrange-Euler inverse dynamic equations in real time. As a result, additional model inaccuracies are introduced if and when simplified versions of the L-E equations are used. Relatively few studies [17] have investigated the robustness of these control schemes to model parameter uncertainty.

It is generally agreed to in the literature that compensation for model inaccuracies is necessary to improve the robustness of model-based controllers. One form of such compensation, among others, is the use of the theory of systems of variable structure (VS) to compute auxiliary (or substitute) control signals. Many attempts in designing robotic VS controllers have relied on neglecting major components of the coupling torques between manipulator joints. Compensation for such torques is often left to the VS controller to achieve. The controller performance, however, can be significantly

improved if estimates of these torques are also fed forward to compensate for them. While some efforts have ignored all components of the coupling torques (gravity as well as inertia and velocity coupling torques) and treated them as disturbances that can be compensated for by the VS controller [1,3,6,9,10], others have relied on direct computation of gravity torques [5] or have made use of the full set of dynamic equations [2,4,7,8]. The latter approach depends on the complexity of the manipulator dynamics and implementation of the control schemes of [2,4,7,8] for manipulators other than the used simple two and three link robots is computationally expensive. Most of the developed VS manipulator controllers have been tested by simulation using very simple (two or three link) robotic structures [1–3,6–10]. By contrast, few efforts have been tested experimentally using actual robot arms [5]. The majority of the reported analyses in this area use continuous time models [1,2,4,6–10] and ignore the effects of friction and damping encountered by the joint motors. Since the robot system is a continuous one that is digitally controlled along a trajectory (or towards a desired position), however, a discretized equivalent (or a sampled data) model of the manipulator is most relevant to this problem.

In this paper, a discretized equivalent model of the continuous robotic system is used at the joint level, taking into consideration all dynamic nonlinearities and sampling effects, to develop a decentralized linear time-varying controller. The motivation for decentralized control is that the developed control algorithms can be executed in parallel using a distributed, relatively inexpensive, architecture while avoiding the burden of computing a global nonlinear manipulator model in real time. Time schedules of the feedback gains and feedforward terms are computed off-line by computing the inverse dynamics along the desired trajectory. Due to uncertainty in some dynamic parameters, however, such as link inertial parameters, some coefficients of the discrete model are not exactly known. These coefficients also change as the robot configuration and load change. This is where the developed controller is modified using a variable structure suction control approach to compensate for model inaccuracies. The approach of this paper makes use of the knowledge of the model form and some of its poles and zeros. This results in a reduction of the number of unknown parameters and more accurate system representation. The developed controller is tested using a multiprocessor architecture and a six joint PUMA 560 robot arm. Each joint is assigned a microprocessor board based on an Intel 8086 processor. The parallel operation of the six processors is synchronized by a common clock. In section 2 of this paper the discrete manipulator model is presented along with the model-based controller. The VS-based controller is developed in section 3. Finally, section 4 presents the experimental testing of the developed controller.

## **2. A Discretized Equivalent Model and a Controller for a Manipulator Joint :**

### **2.1. The Discretized Equivalent Model :**

The discretized equivalent manipulator model developed in [21] is adopted in this paper since it is thought to account for nonlinear arm dynamics, joint motor electrical and mechanical characteristics, damping factors, friction, interference torque between joints, and sampling effects. A block diagram of this model with possible digital compensation and feedback filters is shown in Figure 1. The control voltage,  $V$  is output by each microprocessor joint controller to a digital-to-analog converter (DAC) which acts as a zero order hold (Z.O.H.) device. The DAC output voltage,  $V_{DAC}$ , is applied through a linear voltage amplifier to the joint motor input.  $V_a$  and  $V_m$  are the armature and motor voltages,  $R_a$  and  $L_a$  are the armature resistance and inductance,  $I_a$  is the armature current,  $k_v$  is the motor voltage constant,  $\tau$  is the torque applied by the motor shaft,  $\tau_d$  is the disturbance torque observed at the motor shaft which includes inertia and velocity coupling, gravity, friction, and other disturbance torques,  $J$  is the effective inertia at the motor shaft,  $B$  is the effective damping factor,

$n$  is the gear ratio,  $k'$  is a conversion constant,  $\theta_a$  and  $\theta_d$  are the actual and desired joint positions, and  $\tau'_d$  is a feedforward compensation for  $\tau_d$ . The system inside the dashed line is continuous while the one outside is described by the digital hardware and software used to control the joint.

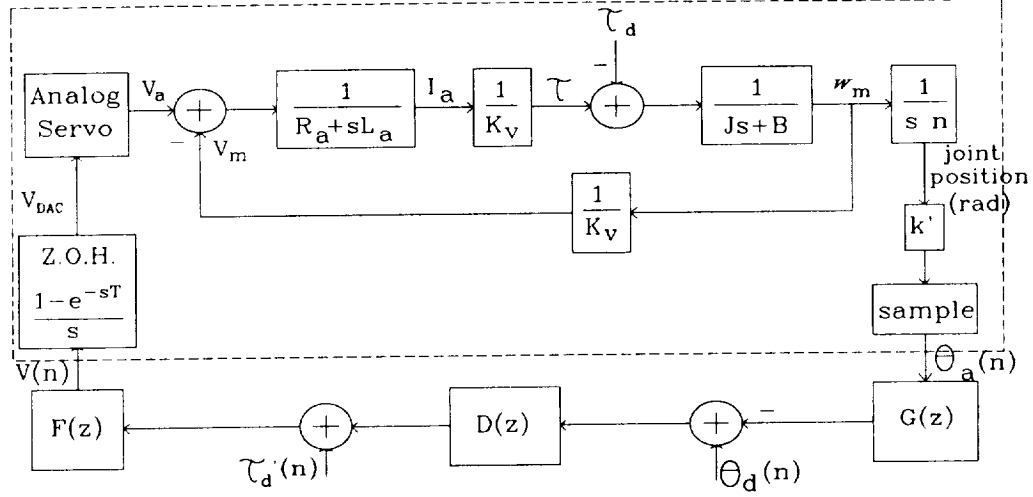


**Figure 1. A Discretized Equivalent Joint Model**

Assuming that  $J$  can be approximated by a constant within each sampling interval, the following transfer functions are obtained [21]

$$H(s) = \frac{\theta_a(s)}{V_{DAC}(s)} \approx \frac{kk'}{nk_v R_a J} \frac{1}{s(s + s_1)} \quad , \quad F'(s) = \frac{\tau_d(s)}{V_{DAC}(s)} \approx \frac{k}{k_v R_a} \quad (1.a)$$

where

$$s_1 = \frac{1}{2} \left[ \left( \frac{B}{J} + \frac{R_a}{L_a} \right) - \sqrt{\left( \frac{B}{J} - \frac{R_a}{L_a} \right)^2 - \frac{4}{k_v^2 L_a J}} \right] \quad (1.b)$$

where the inertia  $J_i$  and disturbance torque  $\tau_d$ , encountered by the rotor of joint  $i$ , are

$$J_i = \frac{D_{ii}}{n_i^2} + J_{r_i} \quad \text{and} \quad \tau_{d_i} = \frac{\tau_i - D_{ii} \ddot{\theta}_i}{n_i} + \tau_{f_i} \quad (2)$$

where  $D_{ii}$  and  $\tau_i$  are the self inertia and torque of joint  $i$  computed using the inverse dynamic equations [15,22],  $J_{r_i}$ ,  $\tau_{f_i}$ , and  $n_i$  are the rotor inertia, friction torque, and gear ratio of joint  $i$ . Using an exact mapping of poles and zeros from the  $s$  plane into the  $z$  plane, ( $z = e^{sT}$ , where  $T$  is the sampling period), the discretized equivalents of the transfer functions (1) are [21]

$$H(z) = \frac{\theta_a(z)}{V_{DAC}(z)} = (1 - z^{-1})Z \left( \frac{H(s)}{s} \right) \approx \frac{k_H z^{-1}(1 + z^{-1})}{(1 - z^{-1})(1 - p_1 z^{-1})} \quad (3.a)$$

$$F'(z) = \frac{\tau_d(z)}{V_{DAC}(z)} = (1 - z^{-1})Z \left( \frac{F'(s)}{s} \right) \approx k_{F'} z^{-1} \quad (3.b)$$

where

$$p_1 = e^{-s_1 T} \quad , \quad k_H = \frac{T k k' (1 - p_1)}{2 n k_v J R_a s_1} \quad , \quad k_{F'} = \frac{k}{k_v R_a} \quad (3.c)$$

where the gains  $k_H$  and  $k_{F'}$  are computed such that the steady state discrete system response is equal to the sampled steady state continuous system response.

## 2.2. The Digital Linear Time-Varying Controller :

Given the transfer functions (3) that represent a manipulator joint, the control task is to design the digital filters  $F(z)$ ,  $D(z)$ ,  $G(z)$ , and a dynamics-based feedforward control signal such that  $\theta_a$  tracks  $\theta_d$  as closely as possible. To perform this task it is necessary here to note the timing of

the model operation. At sample point  $n$  a desired position  $\theta_d(n)$  and an estimated feedforward term  $\tau'_d(n)$  that compensates for  $\tau_d$  are input to the system while the actual joint position  $\theta_a(n)$  is observed. It is desired that the actual position at the next sample time  $(n+1)$  be equal to the desired position input to the system at the current sample time i.e.  $\theta_a(n+1) = \theta_d(n)$ . To achieve this it is necessary to estimate a discrete input,  $\tau'_d(n)$ , that is equivalent to  $\tau_d$  ahead of time to compensate for  $\tau_d$  between the two sample times. This feedforward compensation signal is computed off-line using the robot inverse dynamic equations. Hence, it is desired first to have  $\tau_d(z) = z^{-1}\tau'_d(z)$ . As a result, one gets [21]

$$F(z) = \frac{V(z)}{\tau'_d(z)} = \frac{z^{-1}}{F'(z)} = \frac{1}{k_F'} \quad (4.a)$$

After simple manipulations, the filters  $D(z)$  and  $G(z)$  that result in the response  $\theta_a(z) = z^{-1}\theta_d(z)$  are found to be [21]

$$G(z) = 1 \quad \text{and} \quad D(z) = \frac{k_F'}{k_H} \frac{1 - p_1 z^{-1}}{1 + z^{-1}} \quad (4.b)$$

The feedback control is then written as

$$V(z) = D(z)F(z)[\theta_d(z) - \theta_a(z)] + F(z)\tau'_d(z) \quad \text{with} \quad D(z)F(z) = \frac{1}{k_H} \frac{1 - p_1 z^{-1}}{1 + z^{-1}} \quad (5)$$

In the discrete time domain, the controller is written as

$$V(n) = \frac{1}{k_H^u(n)} [\Delta\theta(n) - p_1^u(n)\Delta\theta(n-1)] + \frac{1}{k_F'} [\tau_d'^u(n) + \tau_d'^u(n-1)] - V(n-1) \quad (6.a)$$

where

$$\Delta\theta(n) = \theta_d(n) - \theta_a(n) \quad (6.b)$$

and superscript  $u$  denotes used (as opposed to actual) values. It remains, however, to compute the feedback gains  $k_H^u(n)$ ,  $p_1^u(n)$ , and  $\tau_d'^u(n)$ . Since the only information available to a joint controller in a decentralized control environment is that generated off-line, estimates of these parameters are computed off-line, when the desired trajectory is generated, and later used in real time to implement the controller (6). This scheme is based on a computed torque approach and, as a result, is susceptible to the potential problems facing a computed torque approach. The most serious problem of these is the difference between the values of  $J$  and  $\tau_d$  along the actual path and their nominal (used) values along the desired path. To address this problem, the controller (6) is modified using the theory of systems of variable structure (VS) to compensate for parameter uncertainty. The modified controller is developed in the next section.

### 3. Development of The Variable Structure Controller :

The purpose of the VS-based controller introduced in this section is to modify the controller (6) such that deviations of the used model parameters from their actual values are compensated for. The basic form of the controller (6) is, however, maintained since it is based on the actual model form which is known. An appropriate sliding surface and a switching variable are selected in terms of the joint tracking error and a suction control strategy [2,4] is used in the discrete time domain to design the controller such that the switching variable and tracking error converge to zero. First, the model (3) is written in the discrete time domain in terms of the actual model parameter values as

$$\begin{aligned} \theta_a(n) = & \theta_a(n-1) + p_1(n-1)[\theta_a(n-1) - \theta_a(n-2)] \\ & + k_H(n-1)[V(n-1) + V(n-2)] - \frac{k_H(n-1)}{k_F'} [\tau_d'(n-1) + \tau_d'(n-2)] \end{aligned} \quad (7)$$

and the switching surface for each joint  $i$  is defined as

$$s(n) = e(n) + \lambda e(n-1) \quad , \quad e(n) = \theta_d(n-1) - \theta_a(n) \quad (8)$$

such that the trajectory tracking error decays exponentially when the switching variable is driven to zero. The switching variable  $s$  is "sucked" to zero using a discretized version of the suction control strategy outlined in the continuous time domain in [2,4]. Namely, the controller is designed so that

$$s(n-1) [s(n) - s(n-1)] < 0 \quad (9)$$

such that  $s(n) > s(n-1)$  if  $s(n-1) < 0$  and  $s(n) < s(n-1)$  if  $s(n-1) > 0$ . Condition (9) is not sufficient for the convergence of  $s(n)$  to zero. If  $|s(n) - s(n-1)|$  can, however, be shown to be bounded by a small positive number  $\delta$  then  $s(n)$  can also be easily shown to be bounded by a small positive number  $\delta'$  using condition (9). To show this, we write

$$\begin{aligned} |s(n) - s(n-1)| &= |e(n) - e(n-1) + \lambda[e(n-1) - e(n-2)]| \\ &= |\theta_d(n-1) - \theta_d(n-2) - [\theta_a(n) - \theta_a(n-1)]| \\ &\quad + \lambda\{\theta_d(n-2) - \theta_d(n-3) - [\theta_a(n-1) - \theta_a(n-2)]\}| \\ &< |\theta_d(n-1) - \theta_d(n-2)| + |\theta_a(n) - \theta_a(n-1)| \\ &\quad + |\lambda| [|\theta_d(n-2) - \theta_d(n-3)| + |\theta_a(n-1) - \theta_a(n-2)|] \\ &< \delta_1 + \delta_2 + |\lambda|(\delta_3 + \delta_4) < \delta \end{aligned}$$

where the magnitude of the upper bound  $\delta$  is determined by the speed of the desired trajectory, the manipulator mechanical time constants, and the sampling frequency. It is clear that  $\delta$  decreases with increasing sampling frequency. For example, if the desired and actual joint speeds are bounded by 10 rad/s and the sampling frequency is 100 Hz, then  $|s(n) - s(n-1)|$  is bounded by 0.25 radians for  $\lambda = 0.25$ . It is clear that as the sampling frequency increases infinitely, condition 10 tends to the suction control condition  $s\dot{s} < 0$  of [4]. Although the condition

$$s(n) [s(n) - s(n-1)] < 0 \quad (9)'$$

is more attractive since it ensures that  $0 > s(n) > s(n-1)$  if  $s(n-1) < 0$  and  $0 < s(n) < s(n-1)$  if  $s(n-1) > 0$ , the design of a controller that would satisfy condition (9)' is quite complicated mathematically (as will be clear from the proof of Lemma 1.). Next, we proceed to design a controller that satisfies condition (9). First, the following set of upper bounds on model parameter deviations is defined

$$\alpha \geq \frac{k_H^u(n)}{k_H(n)} \geq \frac{1}{\alpha}, \quad \alpha \geq 1, \quad \beta \geq |p_1^u(n) - p_1(n)|, \quad \gamma \geq |\tau_d'^u(n) - \tau_d'(n)|, \quad n \geq 0 \quad (10)$$

The variable structure controller that satisfies condition (9) is given by the following lemma.

**Lemma 1 :** The control

$$\begin{aligned} V(n) &= \frac{1}{k_H^u(n)} \left[ \frac{2}{\alpha + 1/\alpha} u_1(n) + \alpha \left( \frac{\alpha - 1/\alpha}{\alpha + 1/\alpha} |u_1(n)| + \beta |\theta_a(n) - \theta_a(n-1)| \right) \operatorname{sgn} s(n) \right] \\ &\quad - V(n-1) + \frac{1}{k_F'} [\tau_d'^u(n) + \tau_d'^u(n-1) + 2\gamma \operatorname{sgn} s(n)] \end{aligned} \quad (11.a)$$

$$\text{where} \quad u_1(n) = \theta_d(n) - \theta_a(n) - p_1^u(n) [\theta_a(n) - \theta_a(n-1)] - (1-\lambda)e(n) - \lambda e(n-1) \quad (11.b)$$

Satisfies the convergence condition (9).

**Proof :** Using the controller (11), the closed loop system response (7) is rewritten as

$$\begin{aligned} \theta_a(n) &= \frac{k_H(n-1)}{k_H^u(n-1)} \frac{2}{\alpha + 1/\alpha} [\theta_d(n-1) - (1-\lambda)e(n-1) - \lambda e(n-2)] \\ &\quad + \left\{ 1 + p_1(n-1) - \frac{k_H(n-1)}{k_H^u(n-1)} \frac{2}{\alpha + 1/\alpha} [1 + p_1^u(n-1)] \right\} \theta_a(n-1) \\ &\quad - \left[ p_1(n-1) - \frac{k_H(n-1)}{k_H^u(n-1)} \frac{2}{\alpha + 1/\alpha} p_1^u(n-1) \right] \theta_a(n-2) \end{aligned}$$

$$\begin{aligned}
& + \alpha \frac{k_H(n-1)}{k_H^u(n-1)} \left( \frac{\alpha-1/\alpha}{\alpha+1/\alpha} |u_1(n-1)| + \beta |\theta_a(n-1) - \theta_a(n-2)| \right) \text{sgn } s(n-1) \\
& - \frac{k_H(n-1)}{k_F'} [\tau_d'(n-1) - \tau_d'^u(n-1) + \tau_d'(n-2) - \tau_d'^u(n-2) - 2\gamma \text{sgn } s(n-1)] \quad (12)
\end{aligned}$$

Using equation (12) and defining the following quantities,

$$\zeta(n) = \frac{k_H(n)}{k_H^u(n)}, \quad \tilde{p}_1(n) = p_1(n) - p_1^u(n), \quad \tilde{\tau}_d'(n) = \tau_d'(n) - \tau_d'^u(n) \quad (13)$$

the increase in the value of the switching variable  $s$  between sample times  $n-1$  and  $n$  is

$$\begin{aligned}
s(n) - s(n-1) &= e(n) - (1-\lambda)e(n-1) - \lambda e(n-2) \\
&= \theta_d(n-1) - \theta_a(n) - (1-\lambda)e(n-1) - \lambda e(n-2) \\
&= \left(1 - \frac{2\zeta(n-1)}{\alpha+1/\alpha}\right) [\theta_d(n-1) - (1-\lambda)e(n-1) - \lambda e(n-2)] \\
&\quad - \left[1 - \frac{2\zeta(n-1)}{\alpha+1/\alpha} + p_1(n-1) - \frac{2\zeta(n-1)}{\alpha+1/\alpha} p_1^u(n-1)\right] \theta_a(n-1) \\
&\quad + \left[p_1(n-1) - \frac{2\zeta(n-1)}{\alpha+1/\alpha} p_1^u(n-1)\right] \theta_a(n-2) \\
&\quad - \alpha\zeta(n-1) \left[ \frac{\alpha-1/\alpha}{\alpha+1/\alpha} |u_1(n-1)| + \beta |\theta_a(n-1) - \theta_a(n-2)| \right] \text{sgn } s(n-1) \\
&\quad + \frac{k_H(n-1)}{k_F'} [\tilde{\tau}_d'(n-1) + \tilde{\tau}_d'(n-2) - 2\gamma \text{sgn } s(n-1)] \\
&= \left(1 - \frac{2\zeta(n-1)}{\alpha+1/\alpha}\right) u_1(n-1) - \tilde{p}_1(n-1) [\theta_a(n-1) - \theta_a(n-2)] \\
&\quad - \alpha\zeta(n-1) \left[ \frac{\alpha-1/\alpha}{\alpha+1/\alpha} |u_1(n-1)| + \beta |\theta_a(n-1) - \theta_a(n-2)| \right] \text{sgn } s(n-1) \\
&\quad + \frac{k_H(n-1)}{k_F'} [\tilde{\tau}_d'(n-1) + \tilde{\tau}_d'(n-2) - 2\gamma \text{sgn } s(n-1)] \\
&= \left(1 - \frac{2\zeta(n-1)}{\alpha+1/\alpha}\right) u_1(n-1) - \alpha\zeta(n-1) \frac{\alpha-1/\alpha}{\alpha+1/\alpha} |u_1(n-1)| \text{sgn } s(n-1) \\
&\quad - \tilde{p}_1(n-1) [\theta_a(n-1) - \theta_a(n-2)] \\
&\quad - \alpha\zeta(n-1) \beta |\theta_a(n-1) - \theta_a(n-2)| \text{sgn } s(n-1) \\
&\quad + \frac{k_H(n-1)}{k_F'} [\tilde{\tau}_d'(n-1) + \tilde{\tau}_d'(n-2) - 2\gamma \text{sgn } s(n-1)] \quad (14)
\end{aligned}$$

Hence,

$$\begin{aligned}
\kappa(n) &= s(n-1)[s(n) - s(n-1)] \\
&= \left[ \left(1 - \frac{2\zeta(n-1)}{\alpha+1/\alpha}\right) \text{sgn } [u_1(n-1)s(n-1)] - \alpha\zeta(n-1) \frac{\alpha-1/\alpha}{\alpha+1/\alpha} |u_1(n-1)s(n-1)| \right. \\
&\quad - [\tilde{p}_1(n-1) \text{sgn } \{s(n-1)[\theta_a(n-1) - \theta_a(n-2)]\} + \alpha\zeta(n-1)\beta] \times \\
&\quad \left. |s(n-1)[\theta_a(n-1) - \theta_a(n-2)]| \right] \\
&\quad + \frac{k_H(n-1)}{k_F'} \{[\tilde{\tau}_d'(n-1) + \tilde{\tau}_d'(n-2)] \text{sgn } s(n-1) - 2\gamma\} |s(n-1)| \\
&= a(n)|u_1(n-1)s(n-1)| + b(n)|s(n-1)[\theta_a(n-1) - \theta_a(n-2)]| + c(n)|s(n-1)| \quad (15)
\end{aligned}$$

and  $\kappa(n)$ ,  $n > 0$ , will be shown to be negative by showing that  $a(n)$ ,  $b(n)$ , and  $c(n)$ , are negative.

1. To show that  $a(n)$  is negative, we need to show that

$$|\alpha + 1/\alpha - 2\zeta(n-1)| < |\alpha\zeta(n-1)(\alpha - 1/\alpha)| \quad (16)$$

Since the right hand side of inequality (16) is positive, two cases are at hand

- a) If  $\alpha + 1/\alpha - 2\zeta(n-1) > 0$ , then we need to show that

$$\alpha + 1/\alpha - 2\zeta(n-1) < \alpha^2\zeta(n-1) - \zeta(n-1)$$

$$\text{or} \quad 1/\alpha - \zeta(n-1) < \alpha[\alpha\zeta(n-1) - 1]$$

$$\text{or} \quad 1 - \alpha\zeta(n-1) < \alpha^2[\alpha\zeta(n-1) - 1]$$

This inequality is satisfied since  $\alpha^2 > \pm 1$ . Hence,  $a(n)$  is negative.

- b) If  $\alpha + 1/\alpha - 2\zeta(n-1) < 0$ , then we need to show that

$$2\zeta(n-1) - \alpha - 1/\alpha < \alpha^2\zeta(n-1) - \zeta(n-1)$$

$$\text{or} \quad \alpha^2[\alpha\zeta(n-1) + 1] > 3\alpha\zeta(n-1) - 1$$

$$\text{or} \quad \alpha^2 > \frac{3\alpha\zeta(n-1) - 1}{\alpha\zeta(n-1) + 1}$$

$$\text{but} \quad \frac{3\alpha\zeta(n-1) - 1}{\alpha\zeta(n-1) + 1} < \frac{3\alpha^2 - 1}{\alpha^2 + 1}$$

$$\text{and} \quad \frac{3\alpha^2 - 1}{\alpha^2 + 1} < \alpha^2$$

$$\text{since} \quad \alpha^4 + \alpha^2 - 3\alpha^2 + 1 = (\alpha^2 - 1)^2 > 0$$

Hence,  $a(n)$  is negative.

2. To show that  $b(n)$  is negative, we need to show that

$$|\tilde{p}_1(n-1)| < \alpha\zeta(n-1)\beta$$

This inequality is satisfied since  $|\tilde{p}_1(n-1)| < \beta$  and  $\alpha\zeta(n-1) > 1$  by definitions (10).

3.  $c(n)$ ,  $n > 0$ , is negative since  $|\tilde{r}'_d(n)| < \gamma$  by definition (10).

Hence, it is seen that  $\kappa(n) < 0$ ,  $n > 0$ , and condition (9) is satisfied.

Q.E.D.

The next section presents the experimental testing of the developed controller.

#### **4. An Example : A PUMA 560 Manipulator :**

To obtain model parameters for a PUMA 560 arm, the motor and armature circuit parameters  $k_v$ ,  $J_r$ , and  $L_a$ , were obtained from the manufacturer.  $R_a$  was measured for each joint by applying a DC voltage at the DAC output and measuring the armature current when no motion took place. To obtain the damping factor and friction torque for each joint a DC voltage was applied at the DAC output and the armature current and joint speed were measured. The resulting data points of current versus speed yielded  $B_i$  and  $\tau_{fi}$  using regression techniques. The linear voltage amplifier gain was set to 4. It was also necessary to adopt a set of link dynamic parameters. There are few reported efforts directed at identifying parameters not supplied by manufacturers such as inertial parameters and centroid coordinates. While some of these efforts adopt direct geometric approaches [22], others rely on experimental identification of these parameters [23–25]. Many approximations are made in [22] about link mass distribution and component shapes. Identification techniques require acceleration, torque, and force sensors and the results often bear a lot of noise [24]. In this paper, link masses were obtained from the manufacturer. Most of the centroid coordinates and inertial parameters reported in [22] were thought to be reasonably accurate and were used. All of the used model parameters for the used PUMA 560 arm are listed in [21].  $\alpha$ ,  $\beta$ , and  $\lambda$  were set to

2, 0.2, and 0.25 respectively for all joints.  $\gamma$  was set to 0.5 N.m for the first three joints and 0.05 N.m for the last three joints.

The desired trajectory for the arm was specified by a cartesian path and a desired velocity profile for the end-effector. The path, sampled every 30 ms, consisted of three curves defined in the arm base frame. The first curve was a semicircle that started at  $(x,y,z)=(15,75,10)$ cm and ended at  $(5,65,-10)$ cm. The point  $(x,y,z)=(10,50,0)$ cm was in the motion plane and the semicircle followed was the one closer to this point. The end-effector accelerated from rest to a velocity of 0.35 m/s in the first 3 segments (90 ms), cruised at this speed for 34 segments, and decelerated to rest in the last 3 segments. The hand approach vector,  $a$ , was required to change from  $(0,0.9798,-0.2)$  to  $(0,0.9798,0.2)$  by requiring the angle

$$\phi = \tan^{-1} \frac{a_z}{\sqrt{1 - a_x^2}}$$

to change from  $-11.5^\circ$  to  $11.5^\circ$  by accelerating in the first 3 segments, cruising at a constant speed in the middle 34 segments, and decelerating to rest in the last 3 segments. The second curve was a straight line that ended at  $(x,y,z)=(-5,85,-15)$ cm. The approach vector,  $a$ , changed to  $(0,0.9539,0.3)$ . All velocity profiles were similar to those of the first curve except for the numbers of acceleration, constant speed, and deceleration segments which were 9, 7, and 9 respectively, and the end-effector constant speed which was 0.48 m/s. The third curve was a semicircle that ended at the initial arm configuration of the first curve. The point  $(x,y,z)=(5,60,-2.5)$ cm was in the motion plane and the semicircle followed was the one closer to this point. All velocity profiles were similar to those of the first curve except for the numbers of acceleration, constant speed, and deceleration segments which were 5, 45, and 5 respectively. The arm stayed at rest for 5 segments between each two curves. The corresponding desired joint trajectories are shown in Figure 2. The used PUMA arm was driven very close to its maximum speed.

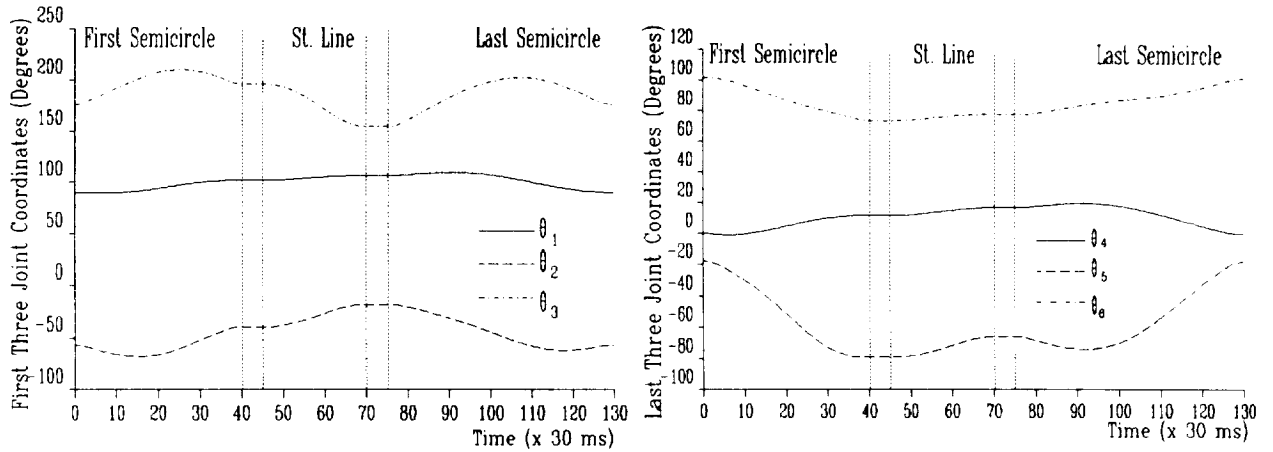


**Figure 2. Desired Joint Trajectories**

The arm was sampled every 10 ms and desired joint positions were generated every 10 ms by linear interpolation between their values stored for use every 30 ms. The feedback gains computed off-line were used three times within the 30 ms intervals each 10 ms (i.e.  $T=0.01$  sec). The computation delay at each sampling interval was 1.00 ms. The joint trajectory tracking errors resulting from this experiment are shown in Figure 3. The tracking error is bounded by 2 degrees for joints 1 and 2, 4 degrees for joint 3, 0.5 degrees for joint 4, 1.5 degrees for joint 5, and 0.25 degrees for joint 6. This performance is slightly worse than that of the controller of [21] which is similar to the controller of this paper except for the absence of the VS-based compensation for model inaccuracy.

One probable cause for the increase in the tracking error, compared to the results of [21], is the chattering problem associated with the VS-based control. This chattering effect is clear in the high frequency behavior of the tracking error of Figure 3 and was felt clearly when the used manipulator exhibited noisy gittery motions during the performed experiments. Another probable cause for the increase in the tracking error is the increase in the computation delay (which is 0.55 ms for the controller of [21]). It does not appear that using a VS-based control, in the experimental context and setup described in this paper, to compensate for model parameter uncertainty has offered an advantage over using parameter estimates computed off-line.

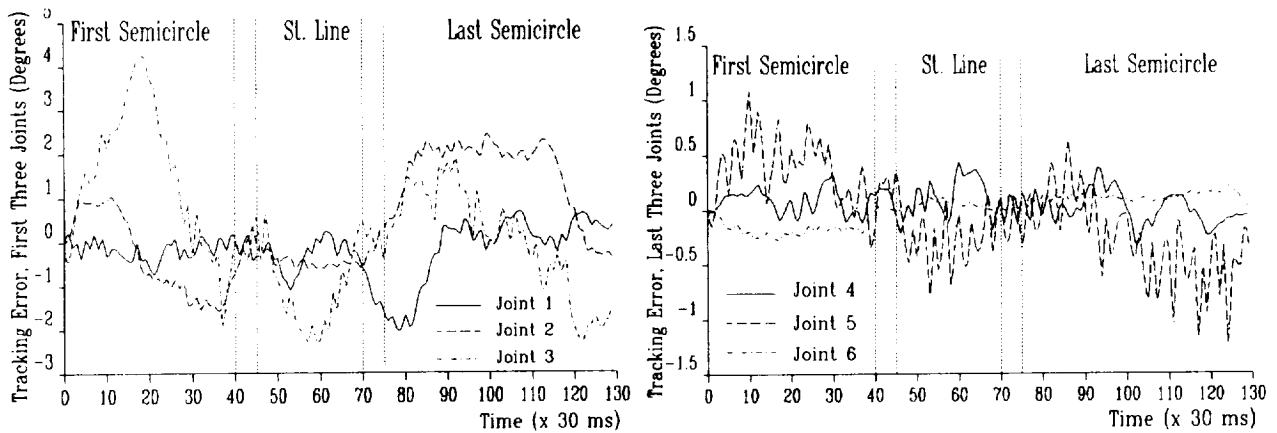


**Figure 3. Joint Tracking Errors**

### **5. Conclusion :**

A decentralized digital linear time-varying variable structure trajectory controller for manipulator arms was developed and tested. A discretized equivalent model of the continuous manipulator system was used to design a nominal digital linear time-varying feedback. Time schedules of the estimated values of the feedback gains and feedforward terms were generated off-line. The feedback was modified using the theory of systems with variable structure to compensate for the difference between the used and actual values of the model parameters. The controller performs reasonably well considering that the used PUMA arm was driven along the trajectory at its maximum speed.

### **References :**

- [1] Young, K., "Controller Design for a Manipulator Using Theory of Variable Structure Systems", *IEEE Tran. Sys. Man & Cyb.*, Vol. SMC-8, No. 2, pp. 210-218, Feb., 1978.
- [2] Slotine, J. and Sastry, S., "Tracking Control of Nonlinear Systems Using Sliding Surfaces, With Application to Robot Manipulators", *Int. J. Con.*, Vol. 38, No. 2, pp. 465-492, 1983.
- [3] Morgan, R. and Özgüner, Ü, "A Decentralized Variable Structure Control Algorithm for Robotic Manipulators", *IEEE J. Rob. Aut.*, Vol. RA-1, No. 1, pp. 57-65, March, 1985.
- [4] Slotine, J., "The Robust Control of Robot Manipulators", *Int. J. Rob. Res.*, Vol. 4, No. 2, pp. 49-64, Summer, 1985.
- [5] Harashima, F. et. al. "Practical Robust Control of Robot Arm Using Variable Structure System", *Proc. IEEE Conf. Rob. & Aut.*, San Francisco, CA, pp. 532-539, April, 7-10, 1986.
- [6] Young, K., "A Variable Structure Model Following Control Design for Robotics Applications", *Proc. IEEE Conf. Rob. & Aut.*, San Francisco, CA, pp. 540-545, April, 7-10, 1986.
- [7] Slotine, J., "On Modeling and Adaptation in Robot Control", *Proc. IEEE Conf. Rob. & Aut.*,

San Francisco, CA, pp. 1387-1392, April, 7-10, 1986.

- [8] Slotine, J. and Coetsee, J., "Adaptive Sliding Controller Design for Nonlinear Systems", *Int. J. Cont.*, Vol. 44, 1986.
- [9] Özgüner, Ü et. al. "Decentralized Variable Structure Control of a Two-Arm Robotic System", *Proc. IEEE Conf. Rob. & Aut.*, Raleigh, NC, pp. 165-168, March, 31-April, 3, 1987.
- [10] Pandian, S. et. al. "A Decentralized Variable Structure Model Following Controller for Robot Manipulators", *Proc. IEEE Conf. Rob. & Aut.*, Philadelphia, PA, 1988.
- [11] Takegaki, M. and Arimoto, S., "An Adaptive Trajectory Control of Manipulators", *Int. J. Cont.*, Vol. 34, No. 2, pp. 291-239, 1981.
- [12] Lim, K. and Eslami, M., "Robust Adaptive Controller Designs for Robot Manipulator Systems", *IEEE J. Rob. Aut.*, Vol. RA-3, No. 1, pp. 54-66, February, 1987.
- [13] Koivo, A. and Guo, T., "Adaptive Linear Controller for Robotic Manipulators", *IEEE Tran. Aut. Con.*, Vol. 28, No. 2, pp. 233-242, 1983.
- [14] Lee, C. and Chung, M., "An Adaptive Control Strategy for Mechanical Manipulators", *IEEE Tran. Aut. Con.*, Vol. 29, No. 9, pp. 837-840, 1984.
- [15] Markiewicz, B., "Analysis of The Computed Torque Drive Method and Comparison with Conventional Position Servo for a Computer Controlled Manipulator", JPL Tech. Memo. 33-601, N73-21198, 1973.
- [16] Freund, E., "Fast Nonlinear Control with Arbitrary Pole Placement for Industrial Robots and Manipulators", *Int. J. Rob. Res.*, Vol. 1, No. 1, pp. 65-78, 1982.
- [17] Ha, I. and Gilbert, E., "Robust Tracking in Nonlinear Systems", *IEEE Tran. Aut. Con.*, Vol. 32, No. 9, pp. 763-771, 1987.
- [18] Leahy, M., and Saridis, G., "The Effects of Unmodelled Forces on Robot Control", *Proc. IEEE 25<sup>th</sup> Conf. Dec. & Con.*, Athens, Greece, pp. 403-408, Dec., 1986.
- [19] Khosla, P., "Some Experimental Results on Model-Based Control Schemes", *Proc. IEEE Int. Conf. Rob. Aut.*, Philadelphia, PA, pp. 1380-1385, April, 24-29, 1988.
- [20] An, C. et. al. "Model-Based Control of a Direct Drive Arm, Part II: Control", *Proc. IEEE Int. Conf. Rob. Aut.*, Philadelphia, PA, pp. 1386-1391, April, 24-29, 1988.
- [21] Tume, Z., "A Gain Scheduling Approach in Decentralized Manipulator Control Using Discretized Equivalent Joint Models", *Proc. 27<sup>th</sup> IEEE Conf. Dec. Con.*, Austin, TX, Dec., 7-9, 1988.
- [22] Paul, R. and Rong, M., "The Dynamics of The PUMA Manipulator", Purdue Univ. Tech. Rep. EE82-34, 1982.
- [23] Olsen, H., and Bekey, G., "Identification of Robot Dynamics", *Proc. IEEE Int. Conf. Rob. Aut.*, San Francisco, CA, pp. 1004-1010, April, 7-10, 1986.
- [24] Atkenson, C., An, C., and Hollerbach, J., "Estimation of Inertial Parameters of Manipulator Loads and Links", *Int. J. Rob. Res.*, Vol. 5, No. 3, pp. 101-119, Fall, 1986.
- [25] An, C. et. al. "Model-Based Control of a Direct Drive Arm, Part I: Building Models", *Proc. IEEE Int. Conf. Rob. Aut.*, Philadelphia, PA, pp. 1374-1379, April, 24-29, 1988.

# **TELEMANIPULATION**

